CopH from *Cupriavidus metallidurans* CH34. A Novel Periplasmic Copper-Binding Protein

Véronique Sendra,[†,‡] Dominique Cannella,[‡] Beate Bersch,[§] Franck Fieschi,[‡] Stéphane Ménage,[∥] David Lascoux,[⊥] and Jacques Covès*[,‡]

Laboratoire des Protéines Membranaires, Laboratoire de Résonance Magnétique Nucléaire, and Laboratoire de Spectrométrie de Masse des Protéines, Institut de Biologie Structurale-Jean-Pierre Ebel, UMR 5075 CNRS-CEA-UJF, 41, rue Jules Horowitz, 38027 Grenoble Cedex, France, and Laboratoire de Chimie et Biochimie des Centres Rédox Biologiques, CEA-Grenoble, DBMS/CB, UMR 5047 CNRS-CEA-UJF, 17 Avenue des Martyrs, 38054 Grenoble Cedex 9, France

Received February 16, 2006; Revised Manuscript Received March 10, 2006

ABSTRACT: The *copH* gene is one of the 19 open reading frames (ORFs) found in the *cop* cluster borne by the large plasmid pMol30 in *Cupriavidus metallidurans* CH34. The entire cluster is involved in detoxification of copper from the cytoplasm as well as from the periplasm. The function of the corresponding protein, CopH, is not yet clear, but it seems to be involved in the late response phase. We have cloned *copH* and overproduced and purified the corresponding protein. CopH is rather unique as only one paralog can be found in the databases. It is a dimeric protein with a molecular mass of 13 200 Da per subunit and located in the periplasm. The metal binding properties of CopH were examined by using a series of techniques such as UV−visible spectroscopy, circular dichroism (CD), electron paramagnetic resonance (EPR), surface plasmon resonance (SPR), mass spectrometry, and nuclear magnetic resonance (NMR). All together, the corresponding data are consistent with a dimeric protein containing one metal-binding site per subunit. These sites have a high affinity for Cu(II) but can also bind zinc or nickel. CopH does not contain any cysteines or methionines but contains two histidines. EPR and UV−visible features are consistent with the presence of Cu(II) type 2 centers in a nitrogen ligand field. SPR data confirm the involvement of the histidine residues in copper binding. CD and NMR data reveal that CopH is partially unfolded.

Because copper is both an essential element for living organisms and a redox-active transition metal, a strict control of its intracellular concentration is required to regulate homeostasis and to manage conditions of copper excess (*1*, and references therein). Genetic determinants for copper homeostasis and resistance exist in a variety of organisms. They include the *pcoABCDpcoRSpcoE* and *copABCDcopRS* loci found in an *Escherichia coli* strain isolated from feces of copper-fed pigs and in the *Pseudomonas syringae* pathovar *tomato* isolated from crop vegetables subjected to copper-based antifungal treatments, respectively (*2*−*5*). The involvement in copper homeostasis of the different elements of the *cop* clusters is relatively well understood for these Gram-negative strains (*1*). For Gram-positive strains, a detailed literature exists for the *copYZAB* operon responsible for copper homeostasis in *Enterococcus hirae* (*6*).

In *Cupriavidus metallidurans* CH34 (formerly *Ralstonia metallidurans* CH34), a facultative autotrophic Gram-negative microorganism characteristic of metal-contaminated biotopes (*7*, *8*), a high level of complexity is reached (*9*). *C. metallidurans* CH34 is exceptionally well equipped to resist high copper concentrations. It contains two clusters related to the *pcoABCDpcoRSpcoE* and *copABCDcopRS* loci. These two clusters have the divergent organization *copSRcopABCD* also found in the related plant pathogen *Ralstonia solanacearum* (*10*). One cluster is located on a megaplasmid, and the second is found on the pMol30 plasmid as part of a large cluster that consists of 19 genes according to a recent reassessment (*11*). Transcriptomic and proteomic data demonstrated that all of the 19 ORFs[1] (*orfV copT orfM copK orfN copSR copABCDI copJGF copL orfQ copH orfE*) of the pMol30 *cop* cluster are differentially expressed when the cells are faced with copper stress (*11*). It has been found that the expression of the individual *cop* genes depends on both Cu(II) concentration and exposure time. A better understanding of the role and the structure of the 19 individual products of the genes constituting the *cop* cluster

[†] V.S. is a Ph.D. fellow of the French National Program of Environmental Nuclear Toxicology.

* To whom correspondence should be addressed. Telephone: 33-(0)4-38-78-24-03. Fax: 33-(0)4-38-78-54-94. E-mail: jacques.coves@ibs.fr.

[‡] Laboratoire des Protéines Membranaires, Institut de Biologie Structurale-Jean-Pierre Ebel, UMR 5075 CNRS-CEA-UJF.

[§] Laboratoire de Résonance Magnétique Nucléaire, Institut de Biologie Structurale-Jean-Pierre Ebel, UMR 5075 CNRS-CEA-UJF.

[∥] CEA-Grenoble, DBMS/CB, UMR 5047 CNRS-CEA-UJF.

[⊥] Laboratoire de Spectrométrie de Masse des Protéines, Institut de Biologie Structurale-Jean-Pierre Ebel, UMR 5075 CNRS-CEA-UJF.

[1] Abbreviations: CD, circular dichroism; EPR, electron paramagnetic resonance; HET-SOFAST HMQC, heterogeneity band-selective optimized-flip-angle short-transient heteronuclear multiple-quantum correlation; HSQC, heteronuclear single-quantum coherence; NMR, nuclear magnetic resonance; ORF, open reading frame; SPR, surface plasmon resonance.

10.1021/bi060328q CCC: $33.50
Published on Web 04/06/2006

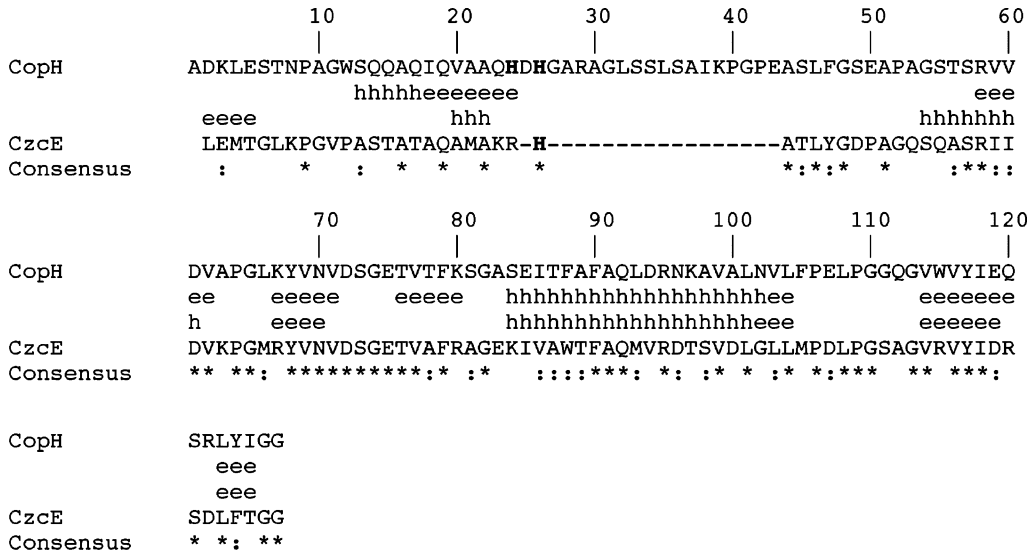

FIGURE 1: Sequence alignment of CopH and CzcE and secondary structure predictions. Asterisks denote identical amino acids, and similarities are identified with colons. Histidines are bold. Secondary structure predictions were obtained by submitting the corresponding sequences to the SOPMA server (*19*) found in the ExPASy tools (http://www.expasy.org/tools/).

is necessary before the question of the interplay of these different actors in the management of copper trafficking can be addressed.

copH is probably involved in the late resistance mechanism as its maximum expression (~100-fold mRNA induction for 0.4 mM copper) occurred after 1 h, while all the other genes were optimally induced 30 min after copper exposition (*11*). In this study, we have overexpressed and characterized CopH, the corresponding protein for which no functional or structural data exist. The only protein found in the databases that is significantly homologous with CopH is CzcE (Figure 1), which is a paralog from *C. metallidurans* CH34. CzcE was identified as a periplasmic metal-binding protein involved in a nonessential metal-dependent induction of the *czc* operon (*12*), itself essential for survival of *C. metallidurans* CH34 at high cobalt, zinc, or cadmium concentrations. It has been postulated that the role of CzcE should be to sense the periplasmic metal cation concentration and then to trigger, by inhibition of the phosphorylation of the regulatory protein CzcS, a signal transduction chain leading to the control of the cytoplasmic *czcNp* promoter. The only histidine residue present in mature CzcE has been shown to be involved in metal binding.

Here we demonstrate that CopH is a dimeric periplasmic protein able to specifically bind two copper ions per dimer with a high affinity. We also show that the two histidine residues of CopH are both involved in copper binding probably along with carboxylates. These data allow us to speculate about the role of this protein in copper homeostasis.

EXPERIMENTAL PROCEDURES

Construction of the Expression Plasmid and Expression and Purification of the Recombinant CopH Protein. The DNA fragment expected to encode the CopH protein devoid of signal peptide was amplified by PCR with suitable restriction sites for subcloning in the pET28a expression vector. The sense primer 5′-AAATTTCCATG**GCTGACAAACTCGAATCCACC** contains the nucleotides (in bold) encoding an N-terminal amino acid sequence starting with alanine 27 (ADKLESTNPAG). The overhanging sequence includes an NcoI site (underlined) carrying the initiator codon ATG. The antisense primer 5′-TTAAAGCTCGAGTCA**ACCGCCGATGTAGAGTCTG** was designed to incorporate an XhoI site (underlined) and a stop codon corresponding to the end of the sequence of CopH. The nucleotides (in bold) are complementary of the corresponding coding sequence of CopH. The authenticity of the DNA insert generated by PCR was confirmed by sequencing. The resulting pET-CopH expression plasmid was used to transform the T7 RNA polymerase-containing host *E. coli* BL21-(DE3). Transformed bacteria from a glycerol stock were grown overnight in 50 mL of LB medium supplemented with kanamycin (50 μg/mL). Then, 1 L of the same medium was inoculated with the overnight preculture. CopH expression was induced at an absorbance of 0.8 at 600 nm by addition of 0.25 mM isopropyl thio-β-galactopyranoside (IPTG). Cells were then grown overnight at 20 °C before being harvested by centrifugation. All subsequent steps were performed at 4 °C. The cell pellet was suspended in a buffer composed of 100 mM Tris-HCl (pH 7.5), 10 mM $MgCl_2$, a small amount of DNase I, and an antiprotease cocktail (Complete, Roche, 1 tablet/50 mL) and lysed by sonic oscillation. The total protein extract was recovered by centrifugation for 90 min at 45 000 rpm in a TI 70 rotor (Beckman) and used for further purification. Residual nucleic acids were eliminated by 2% streptomycin sulfate precipitation. Ammonium sulfate was then used to precipitate soluble proteins, and CopH was found in the pellet obtained at a 50% final saturation. For standard experiments, precipitated proteins were dissolved in a minimal volume of 50 mM Tris-HCl (pH 7.5) (buffer A). The protein solution was subjected to filtration on a Superdex-75 column (Amersham-Pharmacia Biotech) previously equilibrated with the same buffer. Elution was carried out at 0.8 mL/min, and 1 mL fractions were collected. Fractions were assayed for protein (absorbance at 280 nm) and for the presence of CopH (SDS−PAGE analysis). CopH-containing fractions were pooled and concentrated by ultrafiltration using a Diaflo cell equipped with a YM-3 membrane (Amicon Co.) and Centricon-3 microconcentrators. At this stage, CopH was electrophoretically pure and stored at

−80 °C for further use. The yield for a typical purification procedure is more than 150 mg of pure CopH from 1 L of LB medium. When necessary, Tris buffer was exchanged for another buffer by extensive dialysis.

Protein concentrations were determined using bovine serum albumin as a standard and the Micro BCA protein assay (Pierce). The denatured molecular mass of CopH was estimated by 0.1% SDS−15% polyacrylamide gel electrophoresis (*13*), and its native molecular mass was ascertained by elution of a calibrated Superdex-75 filtration column and comparison with the elution volume of chymotrypsinogen A (25 kDa) and ribonuclease A (13.7 kDa).

For the NMR experiments, CopH was purified in the same way after bacteria were grown at 37 °C in M9 minimal mineral medium with glucose (4 g/L) as the carbon source and supplemented with $MnCl_2$ (0.1 mM), $ZnSO_4$ (0.05 mM), $FeCl_3$ (0.05 mM), and a vitamin solution according to the method of Jansson et al. (*14*). Isotopically labeled protein was prepared by growing the cells with $^{15}NH_4Cl$ (1 g/L) as the sole nitrogen source.

Immobilized Metal Affinity Chromatography. A 1 mL chromatography column was packed with Ni−NTA superflow resin (Qiagen), extensively washed with water, and equilibrated with buffer A. CopH (300 μg) was applied to the gel, and the column was washed with 10 mL of buffer A supplemented with 200 mM NaCl. Protein was then eluted with 3 mL of buffer A supplemented with 10 mM EDTA. Fractions (500 μL) were collected and analyzed by SDS−PAGE. After a new extensive washing step with water, the gel was loaded with 3 mL of a 250 mM solution of various other metals ($CuCl_2$, $CoCl_2$, $ZnCl_2$, or $MnCl_2$), and the full procedure was repeated. The protein CopK (*15*) that is specific for copper was used as a control.

Spectroscopic Methods. UV−visible spectra were recorded at room temperature in a quartz cell with a 10 mm light path using a Cary 50 Bio (Varian) spectrophotometer. The cuvette was filled with 1 mL of 0.5 mM CopH in 50 mM Hepes (pH 7.6). A first spectrum corresponding to the apo form of the protein was recorded. Then, small aliquots of copper were added from a freshly prepared stock solution of $CuCl_2$ in water. A spectrum was recorded immediately after each addition. The dilution was considered negligible as the titration of the specific metal binding sites was obtained for a total added volume of 10 μL of $CuCl_2$.

CD spectra were obtained on a Jobin Yvon CD6 spectropolarimeter operating at room temperature. Cells with a path length of 1 mm were used for recording spectra in the UV region (190−260 nm). To study the influence of pH on the protein conformation, 2 μL of 1.7 mM CopH in 50 mM Tris-HCl (pH 7.5) was added to 300 μL of a solution buffered by mixing the required amounts of acidic and basic potassium phosphate at a final concentration of 20 mM. Under these conditions, the final CopH concentration was 11.3 μM. To record the spectrum of Cu-bound CopH, the protein was first diluted to 11.3 μM directly in water, and a reference spectrum was recorded. Then 3 equiv of Cu was added from a freshly prepared concentrated $CuCl_2$ stock solution, and a new spectrum was recorded.

X-Band EPR spectra were recorded with a Bruker EMX spectrometer equipped with an ESR 900 helium flow cryostat (Oxford Instruments). The temperature was set to 20 K. Each sample consisted of CopH at a concentration of 170 μM in Hepes buffer, and the desired amount of $CuCl_2$ was added. Spectra were recorded as described in the legends of the concerned figures.

NMR spectra were recorded at 298 K on a Varian INOVA 600 spectrometer equipped with a triple-resonance (^1H, ^{15}N, and ^{13}C) probe including shielded *z*-gradients. The data were processed using NMR Pipe (*16*), and the spectra were visualized with NMRView (*17*). Samples were prepared with 0.4 mM CopH in MES buffer (pH 6.7), in the absence and presence of 0.9 mM Cu(II). For a semiquantitative determination of protein compactness, $^1H-^{15}N$ HET-SOFAST-HMQC experiments (*18*) were carried out with and without a band-selective inversion pulse, shifted −3 ppm from the water resonance and covering a bandwidth of 4 ppm. One hundred complex points were recorded in the indirect dimension, resulting in an experimental time of approximately 10 min. The ratio of the peak intensities measured in the two spectra ($\lambda_{noe} = I^{sat}/I^{ref}$) is related to the exposure of the corresponding amide group (*18*). λ_{noe} values were determined for the apo form and the Cu(II)-loaded form of CopH.

Surface Plasmon Resonance. SPR experiments were performed using a Biacore 1000 upgrade instrument (Biacore) equipped with a nitrilotriacetic acid (NTA) sensor chip. The machine was primed with the running buffer [10 mM Hepes (pH 7.4), 150 mM NaCl, 50 μM EDTA, and 0.005% surfactant P20], and the NTA chip was loaded with 500 μM $NiCl_2$ as recommended by the manufacturer. CopH was diluted in the running buffer at the required concentrations reported in the corresponding figures legends. All runs were performed at 20 °C and at a flow rate of 30 μL/min. When necessary, the surface was regenerated by a 15 μL injection of 350 mM EDTA at a flow rate of 5 μL/min. For each CopH concentration, a blank was run in parallel on a surface without metal to subtract unspecific binding. For the pH titration, solutions were buffered with Hepes (pH 7.5−7.0), Pipes (pH 6.8−6.1), or Mes (pH 6.0−5.5).

Mass Spectrometry Analysis. Noncovalent (or native) mass spectrometry measurements were performed by using Q-TOF Micro mass spectrometer (Micromass, Manchester, U.K.) equipped with an electrospray ion source. It operated with a needle voltage of 3000 kV and sample cone and extraction cone voltages of 150 and 15 V, respectively. The backing Pirani pressure was set at 10 mbar. The mass spectra were recorded in the 1500−3000 mass-to-charge (*m*/*z*) range. The sample concentration was 10 μM in 50 mM ammonium acetate (pH 6.9) and continuously infused at a flow rate of 5 μL/min. Data were acquired in the positive mode, and calibration was performed using a solution of 1 μM GFP in an acetonitrile/water/formic acid solution (50/50/0.2). Mass spectra were acquired and data processed with MassLynx version 4.0 (Waters).

RESULTS

Overexpression of CopH. A first expression plasmid was constructed with the full-length coding sequence of the *copH* gene, and the corresponding protein was expressed. The SDS−PAGE analysis showed that the overexpressed protein had a molecular mass lower than the expected one (not shown). Thus, the *copH* gene sequence was analyzed to predict post-translational modifications using the ExPASy

proteomics tools (http://www.expasy.org/tools/). A potential signal peptide cleavage site was identified between Ser26 and Ala27, suggesting CopH is a periplasmic protein. Amino-terminal sequencing of the overexpressed protein gave ADKLEST, i.e., a sequence beginning at the predicted cleavage site, thus confirming N-terminal splicing and periplasmic localization of CopH. However, the overexpression yield was poor. To obtain a larger amount of protein, a plasmid containing the DNA fragment encoding a protein without a signal peptide was constructed and CopH was expressed as its mature form in the cytoplasm of *E. coli* BL21(DE3). Maximal overexpression was observed after an overnight culture at 20 °C following addition of IPTG to the growth medium, and CopH was recovered with an excellent yield in the soluble extracts (~25−30% of the total soluble proteins).

Purification and Characterization of CopH. Soluble extracts were first fractionated by ammonium sulfate precipitation. CopH was recovered from the pellet obtained at 50% final saturation and was then further purified to apparent homogeneity by gel filtration on preparative Superdex-75. The final yield was ~150 mg of protein per liter of cell culture. Pure CopH was loaded on a calibrated analytical Superdex-75 column, and its elution volume was compared with those of chymotrypsinogen A (25 kDa) and ribonuclease A (13.7 kDa). CopH and chymotrypsinogen A eluted at the same volume (14.5 mL), while ribonuclease A eluted at 16.4 mL (not shown). As the CopH theoretical molecular mass is 13 201.67 Da, we can conclude that this protein is a dimer in solution. The capacity of CopH to bind divalent metal was tested using metal affinity chromatography. When loaded on Cu(II), Zn(II), and Ni(II) columns, CopH was eluted only with buffer containing EDTA (not shown). However, no binding could be observed when using a Co(II) column. As expected, the CopK protein, used as a control because it is specific for copper (*15*), only bound to the Cu(II) column. This strongly suggests that CopH is a metal-binding protein. As shown in Figure 1, CopH lacks any cysteines and methionines but contains two histidines that can be suspected to be involved in metal binding along with carboxylates.

Analyses of the Metal Binding Capacities of CopH. Mass spectrometry under nondenaturing conditions was used to address the metal binding capacities of CopH. The protein was diluted to 10 μM in ammonium acetate buffer and mixed with increasing amounts of different metals ($CuCl_2$, $ZnCl_2$, or $NiCl_2$) before analysis. Using the soft experimental conditions described in Experimental Procedures, we were able to detect the native dimeric form of CopH (Figure 2A,B) along with the monomeric one (not shown). This is a further demonstration of the dimeric structure of CopH and shows that the two subunits are not linked through covalent interactions. Moreover, the experimentally determined molecular mass of CopH fits the expected mass of the dimeric apoprotein (26 404 Da), showing that pure CopH did not contain any trace of metal. Figure 2A (top trace) shows the mass spectrum of dimeric apo-CopH ions at m/z 2641 (z = 10). Upon addition of 1 equiv of copper (10 μM $CuCl_2$), two extra peaks appear with a mass difference of m/z ~6 and ~12 with respect to the CopH native mass (middle trace). This corresponds to the addition of one and two copper atoms to the CopH dimer, respectively. Concomitantly, the proportion of apo-CopH decreased dramatically. A full conversion

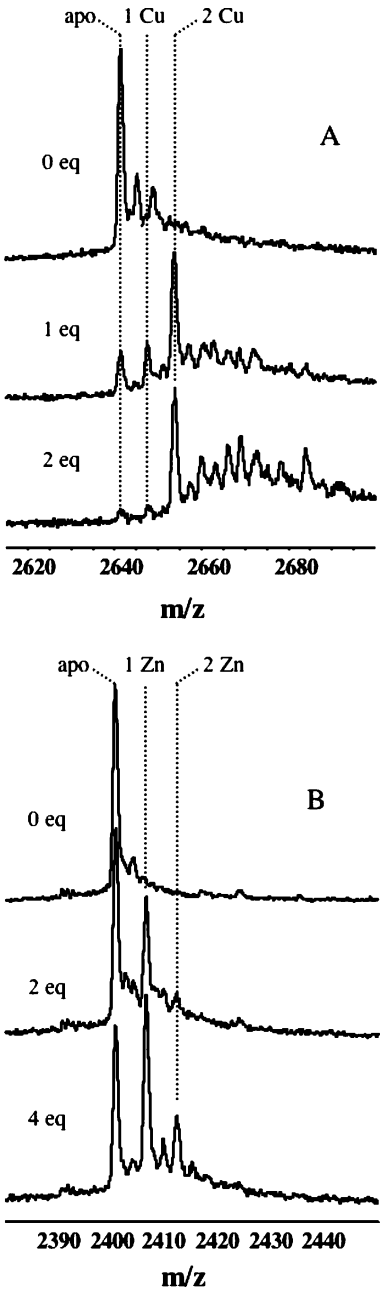

FIGURE 2: ES-MS titration of CopH with $CuCl_2$ or $ZnCl_2$ under native conditions. Only the part of the spectra corresponding to the dimer is shown with a z of 10 in the case of $CuCl_2$ (A) and a z *of* 11 for the addition of $ZnCl_2$ (B). Peaks corresponding to apo-CopH and, to the forms of the protein loaded with 1 and 2 equiv of metal, are indicated. The experimental conditions are described in Experimental Procedures.

to Cu-bound CopH was observed for 2 equiv of copper (20 μM $CuCl_2$). Under these conditions, the peaks corresponding to the apoprotein and the protein with one copper atom were virtually absent, and only the peak corresponding to the binding of two copper ions was apparent (bottom trace). The binding of copper was also observed for the dissociated monomeric form of CopH with similar results (not shown). Upon addition of 0.2 equiv of copper, one extra peak corresponding to the binding of one copper atom appeared along with the peak of the apoprotein. As more copper was added, the proportion of CopH with bound copper increased while the proportion of the apo form decreased until the full conversion observed for 2 equiv of copper, i.e., one copper

ion per subunit. This shows that CopH contains two distinct copper-binding sites, one per monomer, that are not located at the interface of the dimer. $ZnCl_2$ binding and $NiCl_2$ binding were also assayed by mass spectrometry and gave very similar results. Figure 2B shows the mass spectra obtained with $ZnCl_2$. One and two extra peaks appeared upon addition of 2 and 4 equiv of zinc, respectively. These peaks correspond to the binding of one and two zinc atoms, respectively. However, even in the presence of 4 equiv of zinc, the preparation contained a mixture of apo-CopH along with CopH with one or two bound zinc. This strongly suggests a difference in the dissociation constants of copper, zinc, and nickel for CopH. This was definitively demonstrated by a competition experiment. $NiCl_2$ and $CuCl_2$ were chosen for such an experiment because of the difference in the cation molecular mass. CopH was first loaded with Ni(II) by mixing the protein with 10 equiv of $NiCl_2$. Then, 2 equiv of $CuCl_2$ was added, and a native mass spectrum was recorded, showing only the features of copper-bound CopH and thus demonstrating that copper took the place of nickel within the protein (not shown). Competition with glycine was also performed. Two glycines are required to bind one copper atom with a dissociation constant of ~500 nM at pH 7.5 (*20*). However, glycine was able to poorly compete with CopH only when added in a very large excess. The dissociation constant of Cu(II) for CopH is thus significantly lower than 500 nM. The monomer of CopH was also able to bind zinc or nickel (not shown). This common behavior suggests that copper, zinc, and nickel use the same binding sites within the CopH protein.

EPR Characterization of Copper Binding. X-Band EPR measurements were performed to assess the binding of Cu to CopH and the geometry of the binding sites. The results are depicted in Figure 3A. Pure CopH (170 μM in 50 mM Hepes buffer) did not reveal any EPR signal characteristic of Cu(II), showing again that the protein is in its apo form as purified. The EPR spectrum of free copper at a concentration of 340 μM was recorded as a control. Cu(II) in Hepes gives a very slight signal compared to Cu(II) bound to CopH, reflecting the heterogeneity of the solution in copper species in this buffer. Such a phenomenon was very useful for the copper titration experiment. CopH was then titrated with increasing amounts of $CuCl_2$. Only one signal was observed as the amount of Cu(II) increased up to 2 molar equiv. Further addition of Cu(II) led to the appearance of a new signal with EPR parameters close to those of the free Cu(II) sample. Double integration of the low-field hyperfine resonance at 2750 G was plotted as a function of the copper concentration. Figure 3B shows that the signal intensity increases linearly up to 2 equiv of copper and that further addition of this metal did not result in a further increase in the magnitude of this EPR signal. This result confirms the Cu(II)/CopH binding stoichiometry previously deduced from the mass spectrometry experiments. Spectral characteristics were extracted from the spectrum with 2 equiv of Cu(II). The EPR parameters of this signal with a $g_{||}$ of 2.238, a $g_{\perp}$ of 2.053, and a hyperfine coupling of 182 G are compatible with a model of type II copper in a square-planar geometry with a coordination sphere of oxygen or nitrogen atoms. A complex super-hyperfine structure with seven transitions can be extracted from the high-field peak (see the inset of Figure 3B) with an apparent hyperfine constant (a) value of 16 G.

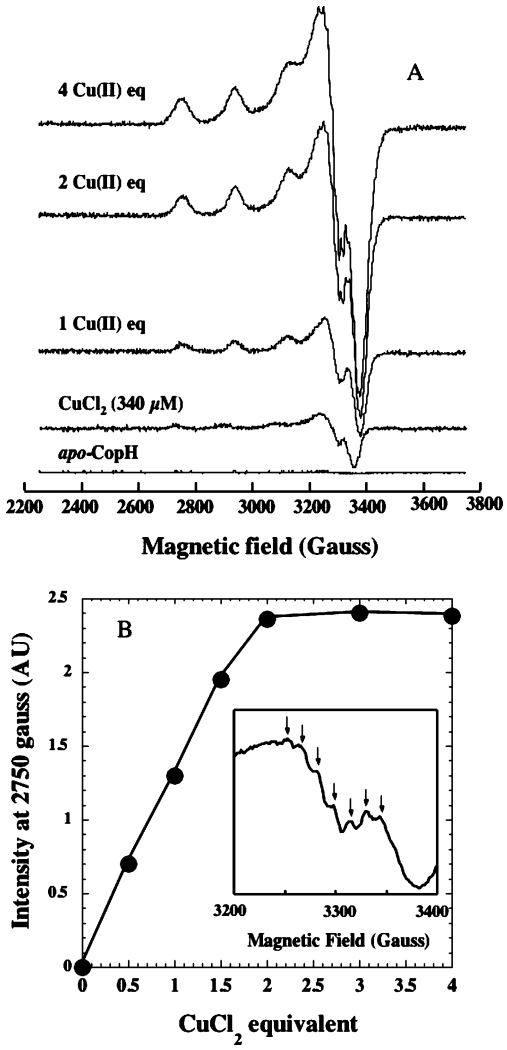

FIGURE 3: X-Band EPR analysis of binding of copper to CopH. (A) The protein was used at a final concentration of 170 μM in Hepes buffer. Copper was added as $CuCl_2$ from a freshly prepared solution in water. As controls, the spectra of apo-copH and of free $CuCl_2$ at a concentration corresponding to 2 equiv of Cu(II) are shown. General conditions are as follows: temperature of 20 K, microwave power of 0.101 mW, microwave frequency of 9.448 GHz, modulation frequency of 100 kHz, and modulation amplitude of 10 G. (B) Plot of the double integration of the low-field hyperfine resonance at 2750 G as a function of the copper concentration, indicating the saturation of the signal for 2 equiv of copper. The inset shows the complex super-hyperfine structure with seven transitions extracted from the high-field peak.

The number of super-hyperfine resonances suggests that there are two nitrogen nuclear spins ($I = 1$) in interaction with the spin of the copper atom with different hyperfine constant values ($a_1 = 16$ G and $a_2 = 8$ G). Therefore, we propose that both His24 and His26 residues are involved in copper binding in CopH but with distinct coordination in terms of the Cu−N distance and/or orientation of the imidazole plane.

Surface Plasmon Resonance Analysis. Surface plasmon resonance (SPR) spectroscopy was used to gain more insight into the metal binding capacities of CopH. All experiments were run with $NiCl_2$ which is the metal recommended by the manufacturer for the best interaction with the NTA sensor chip. Figure 4A shows the dependence on pH of the association of CopH with the Ni−NTA sensor chip. The phase of association run at pH 7.5 confirmed that CopH could bind Ni. During the dissociation phase, the pH was adjusted

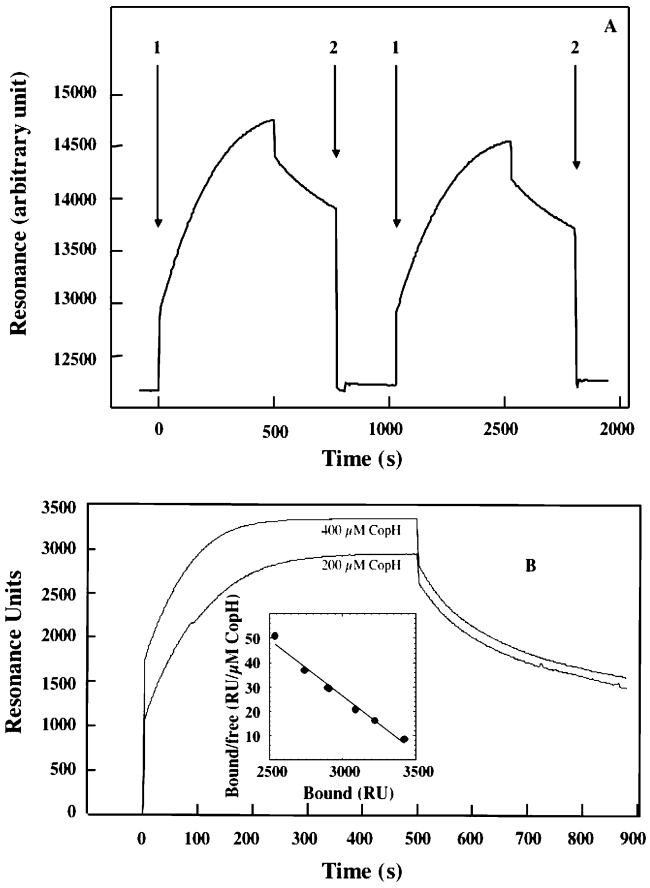

FIGURE 4: SPR analysis of the interaction of CopH with the Ni−NTA sensor ship. (A) Influence of the pH on CopH binding. Apo-CopH (50 μM in 250 μL) was loaded at a rate of 30 μL/min on a Ni−NTA sensor ship at pH 7.5 (arrow 1). During the dissociation phase, the pH was lowered by a pulse addition of Mes buffer (pH 5.5) (arrow 2). After re-equilibration at pH 7.5, the whole experiment was repeated. (B) Determination of the apparent dissociation constant for immobilized nickel. Increasing amounts (from 50 to 400 μM in 250 μL) of CopH were injected at a flow rate of 30 μL/min. After each analysis, the surface was regenerated as described in Experimental Procedures. For simplification, only the results of the injections of 200 and 400 μM CopH are shown. All the data were used for the Scatchard plot analysis shown in the inset.

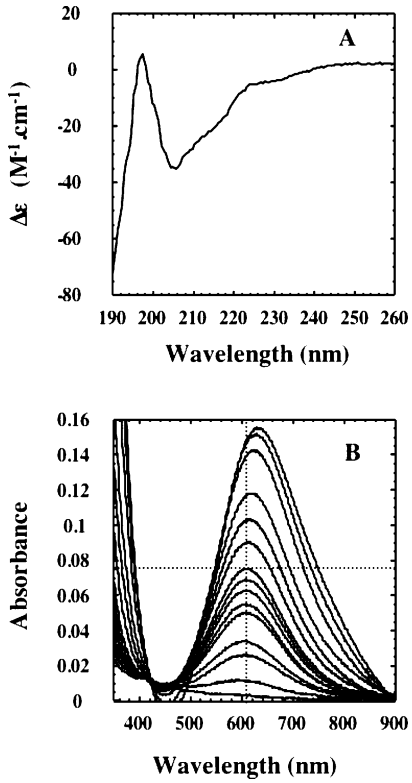

FIGURE 5: CD and UV−visible spectroscopic characterization of CopH. (A) UV (190−260 nm) CD spectrum of apo-CopH in 20 mM potassium phosphate buffer (pH 7.5). (B) UV−visible Cu(II) titration of 0.5 mM CopH in 50 mM Hepes (pH 7.6). A 1 mL cuvette was filled with the protein solution, and the first spectrum was recorded. Stepwise additions of 100 mM $CuCl_2$ were carried out (1, 3, 4, 6, 7, 8, 9, 10, 12, 14, 16, 20, 20, 25, and 30 μL). The absorbance at 610 nm increased linearly up to 10 μL of added $CuCl_2$ (horizontal dotted line), corresponding thus to the addition of 1 mM copper. Further addition of copper led to an absorbance increase characterized by the bathochromic shift illustrated by the deviation from the vertical dotted line.

to 5.5 by replacing Hepes buffer with Mes buffer. CopH fully dissociated instantaneously. After the sensor chip was equilibrated again at pH 7.5, CopH was able to reassociate (Figure 4), showing thus that the previous dissociation was not due to removal of metal from the sensor chip. This result is in agreement with the involvement of histidine residues in copper binding as the dissociation was probably due to histidine protonation at low pH. A pH titration between 7.5 and 5.5 was performed (not shown). Dissociation was observed to start at pH 6.5 and was almost complete at pH 5.8.

SPR was also used to estimate the apparent dissociation constant of CopH for Ni(II). Increasing amounts of CopH were loaded on a Ni−NTA sensor chip under conditions where saturation was obtained at the end of the association phase. Figure 4B shows only the result obtained with 200 and 400 μM CopH as an illustration. Between each CopH loading, the surface was regenerated by a pulse injection of EDTA followed by $NiCl_2$ treatment. Sensorgrams are characterized by an immediate and abrupt increase in resonance followed by an equilibrium phase leading to the saturation of the surface. The dissociation phase starts also by an abrupt decrease in resonance, the amplitude of which is different from that of the abrupt increase. Moreover, the amplitude of both abrupt phases was dependent on CopH concentration. As the binding and dissociation curves did not fit a simple interaction−dissociation model, the kinetic constants could not be determined. However, under these conditions, one can assume that the free CopH concentration corresponds to the protein concentration in the running buffer and that 100% binding corresponds to the saturation expressed in resonance units. These values were used for the Scatchard plot analysis reported in the inset of Figure 4B. An apparent K_d of 20 μM for Ni(II) was deduced from the slope.

Circular Dichroism and UV−Visible Spectroscopic Characterizations. Circular dichroism (CD) studies were conducted in the UV region (190−260 nm) to explore the structural properties of CopH as a function of the pH or of the presence of copper. The recorded spectra remained strictly similar regardless of the pH (7.5 and 5.7) or the presence of 3 equiv of copper at pH 7.5. Figure 5A shows the result obtained at pH 7.5 in the absence of Cu as an example. Analysis of this spectrum using Selcon3 found in Dichroweb (*21*, *22*) suggested that CopH is composed of

21% helix and 24.6% strands. This fits perfectly with the secondary structure prediction shown in Figure 1. According to the Selcon3 analysis, the protein should also contain 38% random coil and 20.2% turn structures. No major conformational changes occurred when the pH was lowered to 5.7, strengthening the hypothesis of the histidine protonation to explain the copper dissociation observed by SPR at acidic pH. In addition, the CD analysis also allows us to conclude that the binding of copper does not significantly affect the secondary structure content of CopH.

Upon addition of copper to CopH, the solution turned instantaneously deep blue. The spectral changes were analyzed between 350 and 900 nm as a function of increasing amounts of $CuCl_2$ added to CopH in Hepes buffer. The results are shown in Figure 5B. Addition of copper first led to the appearance of a large band centered at 610 nm. This absorbance increased linearly up to the addition of 2 equiv of copper with respect to the amount of dimeric CopH protein. Further addition of $CuCl_2$ led to a further increase in absorbance along with a bathochromic shift showing the appearance of a new species. In perfect agreement with the results of the EPR and mass spectrometry analyses, one can deduce that CopH can specifically bind two copper atoms per dimer. From the spectrum of the fully Cu(II)-loaded protein, an extinction coefficient of 150 M^{-1} cm^{-1} at 610 nm can be deduced which is characteristic of a type II Cu(II) d−d transition (*23*).

NMR Spectroscopy. CopH was labeled with ^{15}N, and $^{1}H-^{15}N$ HSQC experiments were recorded at two different pHs. In the spectrum recorded at pH 7.5 (data not shown), only 85−90 peaks over the 119 expected resonances (127 residues minus seven prolines and the N-terminal amino group) could be observed. These resonances display a broad distribution of the NMR frequencies, typical for folded proteins. However, the absence of a large number of expected resonances from the $^{1}H-^{15}N$ HSQC spectrum suggests that the corresponding amino acids are either in slow conformational exchange or highly solvent accessible. Solvent exchange can be slowed by lowering the pH, and indeed, several sharp and intense resonances appear in the center of the spectrum at pH 6.5 (Figure 6A, spectrum shown in black). This indicates the poorly structured nature of the corresponding amino acids. At pH 6.5, roughly 110 peaks can be identified in the $^{1}H-^{15}N$ HSQC spectrum. Additional evidence for the low degree of ordered structure of CopH also comes from the analysis of $^{1}H-^{15}N$ HET-SOFAST correlation experiments (*18*). These experiments were designed for a semiquantitative determination of structural compactness and heterogeneity of proteins in solution and provide measures for the solvent accessibility and proton density at the amide proton sites (*18*). Figure 6B shows the distribution of λ_{noe} values calculated for the 81 $^{1}H-^{15}N$ correlation peaks for which the intensity could be measured with confidence. Low λ_{noe} values indicate a high proton density around the amide proton, which can be related to its localization in a structured protein region. A λ_{noe} distribution as observed for CopH is a typical example for a very heterogeneous protein comprising structured and disordered protein segments (*18*). In this case, one can conclude that roughly 50 amino acids are situated in a well-structured protein core ($\lambda_{noe} \leq 0.4$), which correlates well

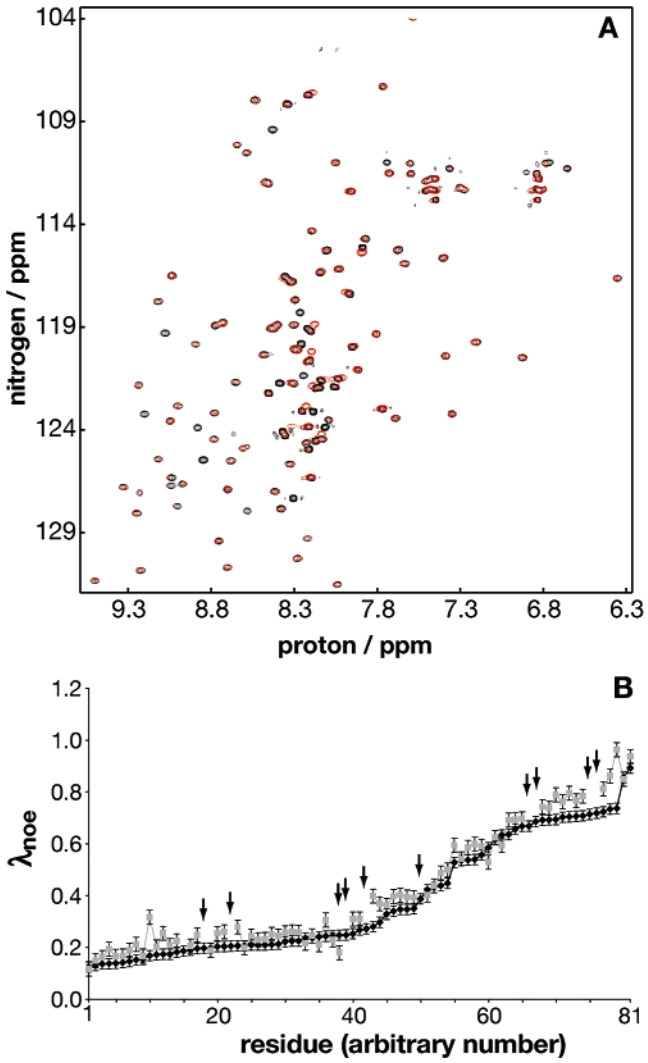

FIGURE 6: NMR characterization of CopH. (A) Superposition of $^{1}H-^{15}N$ HSQC spectra acquired for CopH (0.4 mM) in the absence (black) and presence (red) of 0.9 mM Cu(II). Both spectra were recorded with the same protein sample in 50 mM MES (pH 6.5) at 25 °C. (B) Protein compactness expressed as λ_{noe} determined from the $^{1}H-^{15}N$ HET-SOFAST-HMQC experiment. λ_{noe} is plotted for individual residues (resonance peaks), which are sorted for increasing λ_{noe} values in the apo form of CopH (◆). Low ($\lambda_{noe} \leq 0.35$) values are expected for buried amide groups in the structured part of the protein, whereas a λ_{noe} of ≥ 0.35 indicates increased solvent exposure. Gray squares correspond to λ_{noe} values measured for the same resonance peaks but in the copper-loaded protein. Arrows denote resonances which disappeared upon Cu(II) binding due to paramagnetic line broadening.

with the secondary structure prediction depicted in Figure 1.

Cu(II) is paramagnetic, and the magnetic moment of its unpaired electron affects the NMR parameter of nearby nuclei (*24*). $^{1}H-^{15}N$ HSQC and $^{1}H-^{15}N$ HET-SOFAST experiments were performed to follow the spectral and structural variations due to copper binding. To a freshly prepared CopH sample (0.4 mM) at pH 6.5 was added $CuCl_2$ step by step to a final concentration of 0.9 mM. Figure 6A shows the superposition of the $^{1}H-^{15}N$ HSQC spectra of apo-CopH and copper-bound CopH protein. It can be seen that the addition of Cu(II) to CopH does not induce any major chemical shift changes, confirming that copper binding does not lead to conformational changes. As expected, several

peaks disappear from the spectrum due to the enhanced proton relaxation by the unpaired electron of the nearby Cu(II). The corresponding residues are situated in both the structured and the more flexible part of the CopH protein as shown by the λ_{noe} values measured for the same correlation peaks on the apoprotein. Comparison of the λ_{noe} values of the apo form and the copper-bound form of CopH also demonstrates that copper binding does not lead to a higher degree of ordered structure (Figure 6B).

DISCUSSION

CopH is the product of one of the 19 ORFs found in the *cop* cluster of the *C. metallidurans* CH34 pMol30 plasmid. CopH is an almost unique protein that is significantly homologous only with a paralog from *C. metallidurans* CH34 named CzcE (Figure 1). CzcE was identified as a periplasmic protein that is able to bind to Cu^{2+}, Zn^{2+}, Ni^{2+}, or Co^{2+}−NTA columns. The involvement of the only histidine residue (His24) in metal binding was ascertained by chemical modification with diethyl pyrocarbonate (*12*). We found that CopH also is a periplasmic protein. We have expressed it as its mature form in the cytoplasm of *E. coli*, and large amounts of protein were purified after ammonium sulfate fractionation and gel filtration. The mature form contains two histidine residues in positions 24 and 26 surrounding an aspartate. His26 of CopH can be aligned with His24 of CzcE (Figure 1). CopH was also found to bind to Cu^{2+}, Zn^{2+}, and Ni^{2+} columns but not to Co^{2+}−NTA columns. This prompted us to study the metal binding properties of CopH by different spectroscopic techniques. The protein was first characterized as a dimer by gel filtration and native mass spectrometry. Absorption spectroscopy, EPR, and mass spectrometry showed that CopH was purified in its apo form and was able to bind two metal atoms per dimer with a high specificity for copper. Additional unspecific binding of Cu(II) at higher Cu(II)/protein ratios could be detected but was not further characterized. A full conversion of the apo form to the Cu(II)-loaded form was observed by native mass spectrometry after addition of 2 equiv of copper, while more than 4 equiv of Zn or Ni did not transform CopH to a fully metal-loaded form. Competition experiments between Cu and Zn or Ni demonstrated the specificity for copper, and competition with glycine suggests a low dissociation constant (<500 nM) (*20*). As native mass spectrometry allows detection of both the CopH monomer and the dimer in the same experiment, we could demonstrate that each subunit of CopH contains its own metal binding site. EPR and UV−visible spectroscopies confirmed the metal binding stoichiometry of two copper atoms per dimer of CopH. These two techniques also allowed the characterization of the copper binding sites. Upon Cu(II) binding, CopH turned blue and exhibited a broad absorbance centered at 610 nm. This absorbance characterized by a low extinction coefficient (150 M^{-1} cm^{-1} for the fully loaded protein) is indicative of a type II copper with typical Cu(II) d−d transitions in a nitrogen ligand field (*23*). EPR parameters are in agreement with this conclusion and suggest a coordination sphere of nitrogen and oxygen for copper (*25*, *26*). The involvement of the histidine residues was confirmed by SPR analysis. CopH, able to bind a Ni-loaded sensor ship at pH 7.5, started to dissociate when the pH decreased to 6.5 and fully dissociated at pH 5.8. Knowing that the pK_a for free histidine is 6.04, this relatively large range of pH over which CopH dissociation occurs, suggests that both His24 and His26 residues are involved in Cu(II) binding, each being situated in a distinct environment. This is corroborated by the analysis of the super-hyperfine resonances observed at high field (between 3200 and 3400 G), suggesting different Cu−N distances or geometries for the two histidine residues. The proximity of carboxylates also likely to be involved in copper binding would contribute to the increase in the pK_a of His, resulting in a protonation at higher pH. Moreover, from CD experiments recorded at different pHs, it is clear that dissociation was not due to structural reorganization of the protein. SPR experiments were carried out with nickel. An apparent K_d of 20 μM was deduced for Ni(II) from a Scatchard plot analysis. Even if this value is an upper limit because of the technical conditions (the metal was not in solution but already bound to NTA), it illustrates the difference in affinity found by mass spectrometry between copper and nickel or zinc. CD and NMR spectroscopies were used for a structural characterization of CopH. Both techniques led to the conclusion that this protein is partially unstructured as already suggested by the secondary structure prediction (Figure 1). Compared to CzcE, CopH contains, immediately downstream of His26, an insertion of 17 probably unstructured amino acids. The results of the $^{1}H-^{15}N$ HET-SOFAST-HMQC experiments suggest that CopH is highly heterogeneous with ~30 residues situated in unstructured protein segments. Binding of copper did not induce any significant changes in CopH folding, but the NMR spectral changes reveal that amino acids from both the folded and the unfolded part of the protein are situated in the proximity of the paramagnetic Cu(II) ion (Figure 6A,B). As the protein resonances have not yet been assigned, the corresponding amino acids could not be identified.

CopH is expressed from the *cop* cluster of the *C. metallidurans* CH34 pMol30 plasmid, which is one of the two clusters identified in this strain (*11*), conferring periplasmic copper resistance. Whereas the copper minimal inhibitory concentration (MIC) for a plasmid-free strain containing only the chromosome and the megaplasmid is ~0.6 mM in Tris mineral salts medium, it increases to a value of 1.2 mM in the presence of the pMol30 plasmid (*11*). It appears thus that the *cop* cluster from pMol30 is required for maximal resistance. Moreover, it has been shown by exploring a cosmid library composed of large pMol30 fragments used to complement a plasmid-free derivative that the lack of *copH* led to a slightly lower resistance to copper and a MIC of 0.8−1 mM (ref *11* and personal communication with T. Vallaeys). CopH is thus not essential for resistance to copper but helps to reach the higher levels of resistance. Resistance to copper is a complicated process involving genes from the two different clusters, encoding proteins responsible for periplasmic as well as cytoplasmic copper detoxification. Whereas the function of the proteins belonging to the basic resistance mechanism is quite well characterized (*1*), several genes of the pMol30 cluster encode proteins of completely unknown function for which no or only a few equivalents are found in the protein databases. The proteins encoded by the pMol30 *cop* cluster can be sorted into two main groups: those with methionine-rich motifs and those with cysteine-rich motifs involved in periplasmic or cytoplasmic copper detoxification, respectively (*11*). As demonstrated from quantitative RT-PCR, most of

these genes are highly expressed after incubation of the cells for 30 min in the presence of up to 1 mM Cu(II). CopH is an exception for at least two reasons. The maximum expression of *copH* was observed after 1 h, and the corresponding protein lacks any methionine or cysteine. CopH should thus be involved in a late resistance mechanism, but its exact role is still unknown.

CzcE, the CopH paralog, is supposed to be involved in a nonessential metal-dependent induction of the *czc* operon (*12*) conferring copper, zinc, and cadmium resistance. The regulation of the *czc* operon is quite complex and occurs via the concerted action of several different promoters, probably regulated in the function of the periplasmic and cytoplasmic concentrations of the different metals. It should be noted that two of these metals are essential, whereas the third is purely toxic, which certainly is the reason for the elevated number of regulatory proteins in the *czc* operon (*12*). CzcE has been proposed to be a sensor using the periplasmic cation concentration as a signal for regulating expression of a specific multisubunit efflux pump formed by CzcA, CzcB, and CzcC (*27*). Hence, CzcE would repress *czcNp*, the main in vivo promoter of *czc*, at low periplasmic metal ion concentrations by inhibiting the phosphorylation of CzcS. At higher metal cation concentrations, the signal transduction pathway should lead to the controlled expression of the CzcCBA efflux system. However, this implies that the sensor protein is already present even at low metal cation concentrations and must interact with CzcS. Besides the sequence homology, CopH and CzcE also share a periplasmic localization and belong to a regulon encoding a two-component regulatory system (*28*, *29*). It is therefore tempting to speculate that the physiological role of CopH could be related to the regulation of copper detoxification. It has already been mentioned that the regulation of copper homeostasis acts on two gene clusters, one of which seems to be specialized in the response to high Cu(II) concentrations, with a possible coordination of periplasmic and cytoplasmic copper sensing (*11*). CopH, whose maximal induction is observed 1 h after copper challenge, could be involved in the sensing of periplasmic copper once the detoxification machinery is active and therefore in the regulation of the late response to copper. As also proposed for CzcE, the regulatory function could be performed via an interaction with CopS, thus regulating phosphorylation of CopR (*29*).

Besides this latter hypothesis, CopH could have a very specialized role for copper management. For instance, CopH could be a Cu(II) acceptor from the multi copper-oxidase CopA (*1*, *30*), thus serving to recycle copper-loaded CopA in the periplasm. CopH could also serve for copper trafficking between different Cop proteins, as suspected for CopC (*31*). All the hypotheses suggest an interaction between different partners, and we can speculate that these interactions could be favored by the lack of stable tertiary structure of CopH. Finally, the simplest hypothesis should be that CopH is a copper sequestering protein playing the role of a copper sponge and thus helping the cell to reach the highest capacity of resistance. A more detailed functional and structural characterization of the entire *cop* regulon is needed to decipher the fairly complex interplay between the different proteins that are involved.

ACKNOWLEDGMENT

Max Mergeay and Tatiana Vallaeys were present at the first stage of this study. They are acknowledged for constant encouragement and for making available some information (especially ref *11*). We thank P. Schanda and B. Brutscher for their help with the $^{1}H-^{15}N$ HET-SOFAST-HMQC experiments.

REFERENCES

1. Rensing, C., and Grass, G. (2003) *Escherichia coli* mechanisms of copper homeostasis in a changing environment, *FEMS Microbiol. Rev. 27*, 197−213.
2. Lee, S. M., Grass, G., Rensing, C., Barrett, S. R., Yates, C. J. D., Stoyanov, J. V., and Brown, N. L. (2002) The Pco proteins are involved in periplamic copper handling in *Escherichia coli*, *Biochem. Biophys. Res. Commun. 295*, 616−620.
3. Brown, N. L., Barrett, S. R., Camakaris, J., Lee, B. T., and Rouch, D. A. (1995) Molecular genetics and transport analysis of the copper-resistance determinant (*pco*) from *Escherichia coli* plasmid pRJ1004, *Mol. Microbiol. 17*, 1153−1166.
4. Mellano, M. A., and Cooksey, D. A. (1988) Induction of the copper resistance operon from *Pseudomonas syringae*, *J. Bacteriol. 170*, 4399−4401.
5. Cooksey, D. A. (1994) Molecular mechanism of copper resistance and accumulation in bacteria, *FEMS Microbiol. Rev. 14*, 381−386.
6. Solioz, M., and Stoyanov, J. V. (2003) Copper homeostasis in *Enterococcus hirae*, *FEMS Microbiol. Rev. 27*, 183−195.
7. Vandamme, P., and Coenye, T. (2004) Taxonomy of the genus *Cupriavidus*: A tale of lost and found, *Int. J. Syst. Evol. Microbiol. 54*, 2285−2289.
8. Mergeay, M., Monchy, S., Vallaeys, T., Auquier, V., Benotmane, A., Bertin, P., Taghavi, S., Dunn, J., van der Lelie, D., and Wattiez, R. (2003) *Ralstonia metallidurans*, a bacterium specifically adapted to toxic metals: Towards a catalogue of metal-responsive genes, *FEMS Microbiol. Rev. 27*, 385−410.
9. Noel-Georis, I., Vallaeys, T., Chauvaux, R., Monchy, S., Falmagne, P., Mergeay, M., and Wattiez, R. (2004) Global analysis of the *Ralstonia metallidurans* proteome: Prelude for the large-scale study of heavy metal response, *Proteomics 4*, 151−179.
10. Salanoubat, M., Genin, S., Artiguenave, F., Gouzy, J., Mangenot, S., Arlat, M., Billault, A., Brottier, P., Camus, J.-C., Cattolico, L., Chandler, M., Choisne, N., Claudel-Renard, C., Cunnac, S., Demange, N., Gaspin, C., Lavie, M., Moisan, A., Robert, C., Saurin, W., Schiex, T., Siguier, P., Thebault, P., Whalen, M., Wincker, P., Levy, M., Weissenbach, J., and Boucher, C. A. (2002) Genome sequence of the plant pathogen *Ralstonia solanacearum*, *Nature 415*, 497−502.
11. Monchy, S., Benotmane, A., Wattiez, R., van Aelst, S., Auquier, V., Borremans, B., Mergeay, M., Taghavi, S., van der Lelie, D., and Vallaeys, T. (2006) Transcriptomic and proteomic analyses of the pMol30 encoded copper resistance in *Cupriavidus metallidurans* strain CH34, *Microbiology* (in press).
12. Grosse, C., Anton, A., Hoffmann, T., Franke, S., Schleuder, G., and Nies, D. H. (2004) Identification of a relulatory pathway that controls the heavy-metal resistance Czc via promoter *czcNp* in *Ralstonia metallidurans*, *Arch. Microbiol. 182*, 109−118.
13. Laemmli, U. K. (1970) Cleavage of structural proteins during the assembly of the head of bacteriophage T4, *Nature 227*, 680−685.
14. Jansson, M., Li, Y. C., Jendeberg, L., Anderson, S., Montelione, B. T., and Nilsson, B. (1996) High level production of uniformly ^{15}N- and ^{13}C-enriched fusion proteins in *Escherichia coli*, *J. Biomol. NMR 7*, 131−141.
15. Tricot, C., van Aelst, S., Wattiez, R., Mergeay, M., Stalon, V., and Wouters, J. (2005) Overexpression, purification, crystallization and crystallographic analysis of CopK of *Cupriavidus metallidurans*, *Acta Crystallogr. F61*, 825−827.
16. Delaglio, F., Grzesiek, S., Vuister, G. W., Zhu, G., Pfeifer, J., and Bax, A. (1995) NMRPipe: A multidimensional spectral processing system based on UNIX pipes, *J. Biomol. NMR. 6*, 277−293.
17. Johnson, B. A., and Blevins, R. A. (1994) NMRView: A computer program for the visualization and analysis of NMR data, *J. Biomol. NMR 4*, 603−614.

18. Schanda, P., Forge, V., and Brutscher, B. (2006) HET-SOFAST NMR for fast detection of structural compactness and heterogeneity along polypeptide chains, *Magn. Reson. Chem.* (in press).
19. Geourjon, C., and Deléage, G. (1995) SOPMA: Significant improvements in protein secondary structure prediction by consensus prediction from multiple alignments, *Comput. Appl. Biosci. 11*, 681−684.
20. Dawson, R. M. C., Elliot, D. C., Elliot, W. H., and Jones, K. M. (1986) *Data for Biochemical Research*, Claredon, Oxford, U.K.
21. Lobley, A., and Wallace, B. A. (2001) Dichroweb: A website for the analysis of protein secondary structure from circular dichroism spectra, *Biophys. J. 80*, 373A.
22. Lobley, A., Whitmore, L., and Wallace, B. A. (2002) DICHROWEB: An interactive website for the analysis of protein secondary structure from circular dichroism spectra, *Bioinformatics 18*, 211−212.
23. Solomon, E. I., Lowery, M. D., LaCroix, L. B., and Root, D. E. (1993) Electronic absorption spectroscopy of copper proteins, *Methods Enzymol. 226*, 1−33.
24. Bertini, I., and Pierattelli, R. (2004) Copper(II) proteins are amenable for NMR investigations, *Pure Appl. Chem. 76*, 321−333.
25. Peisach, J., and Blumberg, W. E. (1974) Structural implications derived from analysis of electron-paramagnetic resonance-spectra of natural and artificial copper proteins, *Arch. Biochem. Biophys. 165*, 691−708.
26. Karlin, S., Zhu, Z.-Y., and Karlin, K. D. (1997) The extended environment of mononuclear metal centers in protein structures, *Proc. Natl. Acad. Sci. U.S.A. 94*, 14225−14230.
27. Rensing, C., Pribyl, T., and Nies, D. H. (1997) New functions for the three subunits of the CzcCBA cation−protein antiporter, *J. Bacteriol. 179*, 6871−6879.
28. Munson, G. P., Lam, D. L., Wayne Outten, F., and O'Halloran, T. V. (2000) Identification of a copper-responsive two-component system on the chromosome of *Escherichia coli* K-12, *J. Bacteriol. 182*, 5864−5871.
29. Yamamoto, K., Hirai, K., Oshima, T., Aiba, H., Utsumi, R., and Ishihama, A. (2005) Functional characterization *in vitro* of all two-component signal transduction systems from *Escherichia coli*, *J. Biol. Chem. 280*, 1448−1456.
30. Grass, G., and Rensing, C. (2001) CueO is a multi-copper oxidase that confers copper tolerance in *Escherichia coli*, *Biochem. Biophys. Res. Commun. 286*, 902−908.
31. Arnesano, F., Banci, L., Bertini, I., Mangani, S., and Thompsett, A. R. (2003) A redox switch in CopC: An intriguing copper trafficking protein that binds copper(I) and copper(II) at different sites, *Proc. Natl. Acad. Sci. U.S.A. 100*, 3814−3819.

BI060328Q